LITERATURE CITED

1. W. Hauf and U. Grigul', Optical Methods in Heat Transfer [in Russian], Moscow (1973).
2. Yu. E. Nesterikhin and R. I. Soloukhin, High-Speed Measurement Methods in Gasdynamics and in the Physics of Plasmas [in Russian], Moscow (1967).
3. Merzkirch, in: Methods in Experimental Physics, Vol. 18A: Fluid Dynamics, R. J. Emrich (ed.), New York (1981), pp. 345-403.
4. V. V. Pikalov and N. G. Preobrazhenskii, Reconstructive Tomography in Gasdynamics and in the Physics of Plasmas [in Russian], Novosibirsk (1987).
5. T. O. McCay and J. A. Roux (eds.), Combustion Diagnostics by Nonintrusive Methods, New York (1983).
6. U. Köpf, Opt. Commun., 5, 347-350 (1972).
7. U. Werneking, W. Merzkirch, and N. A. Fomin, 7th All-Union Conference on Heat and Mass Exchange, Minsk, May, 1984. Minsk (1984), Vol. 3, pp. 45-53.
8. N. A. Fomin, U. Werneking, and W. Merzkirch, "Optical methods in dynamics of fluids and solids," in: Proc. IUTAM Symp., Liblice, Czechoslovakia, 1984, M. Pichal (ed.), Berlin (1985), pp. 159-165.
9. U. Werneking, W. Merzkirch, and N. A. Fomin, Experiments in Fluids, 3, 206-208 (1985).
10. R. Jones and C. Wykes, Holographic and Speckle Interferometry, 2nd edn., Cambridge University Press.
11. U. Werneking and W. Merzkirch, Proc. 8th Int. Heat-Transfer Conf., San Francisco, Hemisphere, Washington (1986), pp. 100-105.
12. R. Erbeck and W. Merzkirch, Proc. 1st Symp. on Turbulence, Univ. of Missouri at Rolla (1986), pp. 1-17.
13. G. N. Blinkov, R. I. Soloukhin, and N. A. Fomin, Problems of Heat and Mass Exchange, 1986 [in Russian], Minsk (1986), pp. 92-97.
14. G. N. Blinkov, D. É. Vitkin, and N. A. Fomin, "Contemporary experimental methods of research into the processes of heat and mass exchange," in: Proceedings of the International School Seminar (Minsk, May, 1987), Minsk (1987), Ch. 1, pp. 28-35.
15. G. N. Blinkov, D. É. Vitkin, R. I. Soloukhin, and N. A. Fomin, Dokl. Akad. Nauk BSSR, 31, No. 10, 895-898 (1987).

FLOW IN THE INITIAL SEGMENT OF A TUBE WITH A SHARP INLET EDGE. COMPARATIVE ANALYSIS

V. M. Legkii and V. A. Rogachev

UDC 532.526

When flow becomes detached in the inlet segments of tubes and channels with sharp leading edges and where the Reynolds numbers exceed $75 \cdot 10^3$, the displacement of the maximum of the local heat transfer is in agreement with the onset of secondary laminar flow.

The detached flow model proposed in [1] can be compared with experimental heat-exchange and friction data applicable to the initial segments of tubes and channels with sharp inlet edges; this comparison is carried out on the basis of direct measurements of the surface static pressures and on the basis of the results from studies into local heat exchange, which can be found in [2-5].

For purposes of determining surface static pressures on a bench, such as that used in experiments to achieve flow visualization [1], we mounted a one-piece initial segment 80 mm in length ($X/d_{eq} = 2.22$) with a system of drainage orifices whose inside diameter was 0.5 mm. The curve of the changes in surface statistical pressure along the longitudinal coordinate for $Re_{d_{eq}} = 78 \cdot 10^3$ is shown in Fig. 1. The figure shows the positions of the

Kiev Polytechnic Institute. Translated from Inzhenerno-Fizicheskii Zhurnal, Vol. 56, No. 4, pp. 547-550, April, 1989. Original article submitted September 29, 1987.

0022-0841/89/5604-0381$12.50

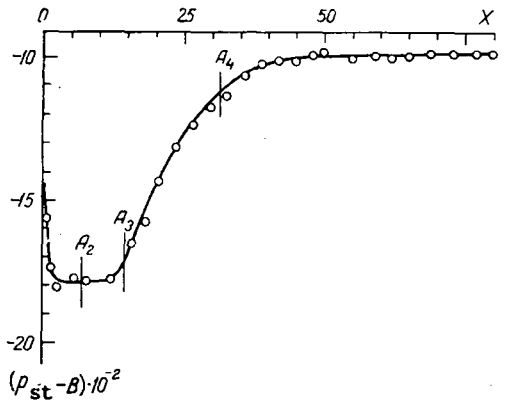

Fig. 1

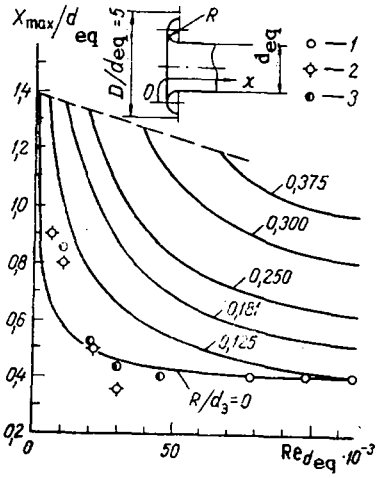

Fig. 2

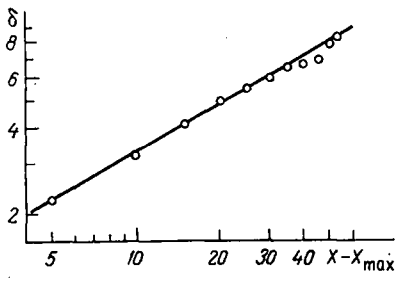

Fig. 3

Fig. 1. Distribution of surface static pressures along the longitudinal coordinate in the initial section of the tube with a sharp leading edge, $Re_{d_{eq}} = 78\cdot10^3$, B = 0.1 MPa. T_{flow} = 296 K, p_{st} − B, Pa.

Fig. 2. The coordinate of the maximum heat transfer in the initial segments of the tubes and channels as a function of the Reynolds number and of the curvature radius of the inlet edge, according to [2, 3]: 1) according to the visualization data from [1]; 2) according to the data of [4]; 3) according to the data of [5].

Fig. 3. The thickness of the secondary-flow boundary layer as a function of the longitudinal coordinate in the case of $Re_{d_{eq}} = 78\cdot10^3$. $X - X_{max}$, mm.

characteristic cross sections A_2, A_3, and A_4, where, on the basis of the visualization result (see Fig. 3 in [1]), we find, respectively, the right edge of the vortex, the onset of secondary flow in the detached region near the wall, and the point with zero velocity at the wall. As follows from [1], the coordinates of sections A_2 and A_3 are constant through the interval $Re_{d_{eq}} = (78\text{-}115)\cdot10^3$ and amount to $X_2/d_{eq} = 0.28$, $X_3/d_{eq} = 0.42$, whereas the coordinate of section A_4 increases monotonically together with the Reynolds number, following the relationship $X_4/d_{eq} \approx 0.115Re_{d_{eq}}^{0.18}$, which is a consequence of the rotational acceleration of the vortex.*

The minimum of the statistical pressure is situated in Fig. 1 virtually at the center of the area occupied by the vortex, while the intensive restoration of the pressure begins markedly earlier than the secondary flow. No specific unique features which would enable us to identify section A_4 can be observed in the distribution of the pressures. The indicated circumstances lead us to the conclusion that the measurement of the surface pressures

*According to the data shown in Fig. 1, the inlet drag coefficient amounts to $\zeta = 0.51$, which coincides with the handbook values.

is inadequately informative with regard to the mechanism of detached flow and, apparently, only in very small measure reflects the pattern of the three-dimensional field of static pressures in the initial segment.

The extremum of local heat-exchange intensity which appears in flows that become detached in the initial segment of tubes and channels, based on the model taken from [1], should be associated with section A_3, since to the left of this section, all the way to the start of the vortex zone in section A_2, the thickness of the layer with reverse motion at the wall increases, while to the right of this section we note a rapid increase in the thickness of the secondary-flow region. Figure 2 shows curves taken from [3] for the determination of the coordinate of the maximum for the local coefficient of heat exchange in the initial segments of the tubes and channels, as a function of the Reynolds number and of the curvature radius of the inlet edge. These curves have been plotted in [3] on the basis of the experimental data on the longitudinal distributions of local heat-exchange coefficients in rectangular channels and confirmed experimentally [2] in a round tube. The curve for $R/d_{eq} = 0$ in the lower part of the figure pertains to the case of a sharp inlet edge with an angle of 90°. The dashed line intersects the region of the values of $Re_{d_{eq}}$ and R/d_{eq}, beyond whose limits the detachment maximum in heat-exchange intensity in the initial segments is no longer tracked. As we can see from Fig. 2, the detachment maximum in local heat transfer in the inlet segments of the tubes and channels with sharp leading edges exists even with Reynolds numbers of $Re_{d_{eq}} = (8\text{-}10)\cdot 10^2$, considerably smaller than the critical value, while the coordinate of section A_3, in which the secondary flow begins, found from the visualization data of [1], are in entirely satisfactory agreement with the displacement of the maximum when $Re_{d_{eq}} > 75\cdot 10^3$.

A number of experimental points have been plotted in Fig. 2 on the basis of experimental results from the initial segment of the rectangular channel with a sharp leading edge, as published in [4, 5]. The curves for $\alpha_{loc} = f(X)$ were plotted in [4, 5] for the heat-exchange coefficients averaged over the lateral direction, which should result in some distortion of the function $X_{max}/d_{eq} = f(Re_{d_{eq}})$ as a consequence of the nonequivalence of the corner zones for various Reynolds numbers. However, on the whole the results of [4, 5] correlate satisfactorily with the curve $X_{max}/d_{eq} = f(Re_{d_{eq}})$ for $R/d_{eq} = 0$. It is useful to point out that the heat-transfer intensity measurements in [2] were carried out with built-in standard-regime alpha calorimeters; these measurements were carried out in [3] by means of internal Gerashchenko heat-flow sensors, while in [4, 5] the measurements were accomplished with the naphthalene sublimation method.

Since the visualized observations give evidence in favor of a laminar nature for the secondary flow, at least in the initial segment $X/d_{eq} < 2$, it becomes essential to track the quantitative relationship governing the increase in the thickness of the boundary layer beyond the section A_3 (i.e., to the right of the maximum of the local heat-exchange intensity). Figure 3 shows the thickness of the boundary layer in the secondary flow as a function of the coordinate $X - X_{max}$. The values of δ have been found from the photographs in [1] with $Re_{d_{eq}} = 78\cdot 10^3$, while the coordinate X_{max} is taken from Fig. 2. The averaging line in Fig. 3 has a slope of 0.55, which is only slightly higher than in the case of laminar streamlining of a plate with a parabolic Blasius velocity profile at the wall. If we bear in mind that beyond section A_3 the velocity profiles in the secondary flow differ by the presence of a bend, and that directly within section A_3 (i.e., when $X - X_{max} = 0$) the thickness of the boundary layer is not equal to zero and motion within its limits is reversed relative to the direction of the main flow, then the differences relative to the results from the Blasius solution may be regarded as fully validated.

In the light of the considerations expressed above, the experimental material with regard to the local exchange of heat beyond the heat-transfer maximum in the initial segments of those tubes and channels with sharp inlet edges at high Reynolds numbers are expediently processed within a system of determining parameters, such as those that are assumed for laminar flows, and here we might expect that in the interval of small and moderate $Re_{d_{eq}}$, smaller than $30\cdot 10^3$, the absolute values of the local heat-exchange coefficients beyond the maximum will drop below the level corresponding to developed turbulent flow. This is borne out, in particular, by the trends observed in [6].

NOTATION

X, the longitudinal coordinate, mm; d_{eq}, the equivalent diameter of the channel flow-through section, mm; δ, the thickness of the secondary boundary layer, mm; D, the diameter of the face flange, mm; R, the curvature radius of the inlet edge, mm; B, the barometric pressure, Pa; p_{st}, the surface static pressure, Pa; T_{flow}, the temperature of the air that is drawn in, K; $Re_{d_{eq}}$, the Reynolds number calculated on the basis of the average flow rate. Indices: 2, 3, 4, section number; max, maximum; flow, flow.

LITERATURE CITED

1. V. M. Legkii and V. A. Rogachev, Inzh.-Fiz. Zh., 56, No. 2, 215-220 (1980).
2. V. D. Burlei, "Investigating the exchange of heat and flow in the initial segments of circular tubes," Dissertation, Candidate of Technical Sciences, Kiev (1982).
3. A. S. Makarov, "Certain quantitative relationships governing the flow and transfer of heat in the initial segments of rectangular channels," Dissertation, Candidate of Technical Sciences, Kiev (1970).
4. E. M. Sparrow and N. Kern, Teploperedacha, 105, No. 3, 100-109 (1983).
5. E. M. Sparrow and N. Kern, Teploperedacha, 104, No. 1, 89-97 (1982).
6. V. M. Legkii and V. D. Burlei, Prom. Teplotekhn., 7, No. 1, 6-9 (1985).

APPLICATION OF THE LARGE-SCALE PARTICLE METHOD IN INVESTIGATING THE EXCHANGE OF HEAT BETWEEN A GAS AND PARTICLES IN TWISTED-FLOW COUNTERCURRENT APPARATUS

É. F. Shurgal'skii

UDC 532.529

The model of interpenetrating continua serves as the basis for an investigation into the exchange of heat between a carrier and dispersion phase. It is demonstrated that the exchange of heat increases the efficiency with which dust is collected in vortex-type equipment.

Twisted-flow countercurrent dust collectors (TCDC) occupy a unique place in the technology of dust collection. These collectors are characterized by a high level of dispersed impurity removal from the gases, as well as by their limited sensitivity in purification efficiency to oscillations in the flow rates of the gas and particles at the inlet sections, by the absence of abrasive wear on the inside surfaces of the equipment, etc. In this connection, such equipment is presently being introduced on a broad scale into various branches of industry.

The hydrodynamics of gas suspensions in TCDC has been studied rather fully in [1, 2]. Here, as in many other references, it is assumed that the temperature of the gas and of the particles at the inlet to the equipment is identical. However, in many industrial lines, primarily in those in which the dispersion phase is dried with a hot gas, the temperatures of the gas and of the particles at the inlet to the TCDC will differ significantly, and this difference may bring about a change in the structure of flow interaction within the apparatus as a consequence of heat exchange between the phases.

1. Formulation of the Problem. Let us examine the interaction of two twisted flows in a cylindrical area whose longitudinal cross section can be seen in Fig. 1. In this figure AL denotes the axis of symmetry, while the lines BCDE and MN identify the solid walls. A preliminary twisted flow, containing the particles of the dispersion phase, is passed through the section AB. At the other end, through the circular section ME, we have the secondary

Moscow Chemical Machine-Building Institute. Translated from Inzhenerno-Fizicheskii Zhurnal, Vol. 56, No. 4, pp. 550-555, April, 1989. Original article submitted April 25, 1988.

0022-0841/89/5604-0384$12.50